



## A rare case of solution and solid state inter-conversion of two copper(II) dimers and a copper(II) chain

Subrata Naiya<sup>a,b</sup>, Saptarshi Biswas<sup>a</sup>, Michael G.B. Drew<sup>c</sup>, Carlos J. Gómez-García<sup>d,\*</sup>, Ashutosh Ghosh<sup>a,\*</sup>

<sup>a</sup> Department of Chemistry, University College of Science, University of Calcutta, 92, APC Road, Kolkata 700 009, India

<sup>b</sup> Susil Kar College, Ghoshpur, Champahati, Baruipur, 24 Parganas(S), West Bengal 743 330, India

<sup>c</sup> School of Chemistry, The University of Reading, P.O. Box 224, Whiteknights, Reading RG 66AD, UK

<sup>d</sup> Instituto de Ciencia Molecular (ICMol), Parque Científico, Universidad de Valencia, 46100 Paterna, Valencia, Spain

### ARTICLE INFO

#### Article history:

Received 9 May 2011

Received in revised form 9 July 2011

Accepted 19 July 2011

Available online 4 August 2011

#### Keywords:

Copper(II)

Schiff base

Antiferromagnetic

Crystal transformation

$\mu$ -1,1 Single azido bridged

### ABSTRACT

Three Cu(II)-azido complexes of formula  $[\text{Cu}_2\text{L}_2(\text{N}_3)_2]$  (**1**),  $[\text{Cu}_2\text{L}_2(\text{N}_3)_2]\cdot\text{H}_2\text{O}$  (**2**) and  $[\text{CuL}(\text{N}_3)]_n$  (**3**) have been synthesized using the same tridentate Schiff base ligand HL (2-[(3-methylaminopropylimino)-methyl]-phenol), the condensation product of *N*-methyl-1,3-propanediamine and salicylaldehyde). Compounds **1** and **2** are basal-apical  $\mu$ -1,1 double azido bridged dimers. The dimeric structure of **1** is centrosymmetric but that of **2** is non-centrosymmetric. Compound **3** is a  $\mu$ -1,1 single azido bridged 1D chain. The three complexes interconvert in solution and can be obtained in pure form by carefully controlling the synthetic conditions. Compound **2** undergoes an irreversible transformation to **1** upon dehydration in the solid state. The magnetic properties of compounds **1** and **2** show the presence of weak antiferromagnetic exchange interactions mediated by the double 1,1- $\text{N}_3$  azido bridges ( $J = -2.59(4)$  and  $-0.10(1) \text{ cm}^{-1}$ , respectively). The single 1,1- $\text{N}_3$  bridge in compound **3** mediates a negligible exchange interaction.

© 2011 Elsevier B.V. All rights reserved.

### 1. Introduction

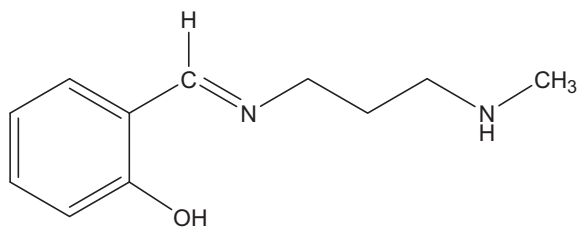
In recent years, the synthesis of polynuclear complexes of Schiff base ligands with polyatomic anions has witnessed a huge advance thanks to their interesting applications in the field of structural chemistry [1–5], magnetism [1–3,6–9], gas storage [10–12], catalysis [13] and luminescence [14,15]. The steric and electronic effects of the Schiff base as well as the polyatomic bridging ligand play a crucial role in constructing the polymeric structure. Among the different transition metal and anions used, the Cu(II)-azide system is the most popular one. A variety of copper–azido complexes with discrete monomeric or one-, two-, and three-dimensional polymeric structures have been reported, in which the azido ligand exhibits diverse bridging modes ranging from  $\mu$ -1,1 (end-on, EO) and  $\mu$ -1,3 (end-to-end, EE) to  $\mu$ -1,1,1,  $\mu$ -1,1,3,  $\mu$ -1,1,1,1,  $\mu$ -1,1,3,3, and  $\mu$ -1,1,1,3,3,3, depending upon the steric and electronic demands of the co-ligands [16–24]. Among the various bridging modes of the azide ion,  $\mu$ -1,1 (end-on, EO) is the most common one and can be either basal–basal [25,26] or basal–apical [27–30]. In the literature, the basal–basal and basal–apical coordination are usually termed respectively as symmetric and unsymmetric (or asymmetric) bridging. It may be found that when the blocking li-

gand is chelating tridentate, the azide ligand bridges adjacent copper(II) centres acting as a basal–apical bridge [27–30]. Regarding the basal–basal bridging mode, it has been established that when the azido ligand bridges two Cu(II) ions in a  $\mu$ -1,1 manner, the nature of the exchange coupling changes from ferromagnetic to antiferromagnetic when the Cu–N–Cu angle increases, with a crossing point at around  $108^\circ$  [25,26,31]. In contrast, basal–apical bridges usually give rise to very small magnetic couplings since the magnetic orbital containing the unpaired electron is mainly of an  $x^2 - y^2$  type lying in the basal plane of the copper atoms with an almost negligible contribution on the axis perpendicular to the basal plane. For such small coupling, the Cu–N–Cu angle is not indicative of the magnetic interaction. Instead, several other factors, such as the steric and electronic factors of the blocking ligand, the Addison parameter,  $\tau$ , the axial Cu–N bond distances, supramolecular H-bonding interactions, etc. play an important role in controlling the magnitude and sign of the coupling constants [30] and therefore, contrary to their basal–basal analogues, there is no clear magneto-structural correlation. To have a better insight into the magnetic properties of these complexes, the synthesis of different compounds using the same blocking ligand seems necessary, although optimization of the synthetic conditions in order to obtain the different compounds in pure form is still a challenge.

Herein, we present the syntheses, crystal structures, and variable-temperature magnetic properties of three basal–apical azido bridged compounds,  $[\text{Cu}_2\text{L}_2(\text{N}_3)_2]$  (**1**),  $[\text{Cu}_2\text{L}_2(\text{N}_3)_2]\cdot\text{H}_2\text{O}$  (**2**)

\* Corresponding authors.

E-mail address: ghosh\_59@yahoo.com (A. Ghosh).



Scheme 1. Schiff base ligand HL.

and  $[\text{CuL}(\text{N}_3)]_n$  (**3**). These three derivatives have been prepared using azide and a single N,N,O donor Schiff base ligand, 2-[(3-methylaminopropylimino)-methyl]-phenol (HL, Scheme 1). Both **1** and **2** are double asymmetric  $\mu$ -1,1-azide bridged dimers; the only difference in their composition is that **2** contains a water of crystallization. Compound **3** is a rare example of a single asymmetric  $\mu$ -1,1-azido bridged polymer. All three complexes interconvert in solution. The factors that allow the conversion of one compound into another in solution have been explored. Compound **2** undergoes an irreversible solid state transformation to compound **1** upon dehydration. During the course of this work, the crystal structures of **3** and a compound related to **2** in which methanol was the solvent molecule have been reported by others [28]. However, the previous authors reported only the synthesis and crystal structures of the compounds. The inter-conversion of the compounds in solution, the solid-state transformation of **2** to **1** and the magnetic properties were not reported.

## 2. Experimental

**Materials:** The reagents and solvents used were of commercially available reagent quality.

### 2.1. Synthesis of the Schiff base ligand 2-[(3-methylaminopropylimino)-methyl]-phenol (HL)

The monocondensed Schiff base ligand HL (Scheme 1) was synthesized by the condensation of salicylaldehyde (1.05 mL, 10 mmol) and *N*-methyl-1,3-propanediamine (1.04 mL, 10 mmol) in methanol (10 mL) as reported earlier [5]. The resulting dark yellow solution was then used directly for complex formation.

### 2.2. Synthesis of $[\text{Cu}_2\text{L}_2(\text{N}_3)_2]$ (**1**)

$\text{Cu}(\text{ClO}_4)_2 \cdot 6\text{H}_2\text{O}$  (0.582 g, 2 mmol), dissolved in 10 mL of methanol, was added to a methanolic solution (10 mL) of the ligand (HL) (2 mmol) with constant stirring. After 10 min, a methanol-water solution (9:1, v/v) of  $\text{NaN}_3$  (0.130 g, 2 mmol) was added. The colour of the solution turned to deep blue. By slow evaporation of the resulting solution at room temperature, blue coloured X-ray quality, rectangular shaped single crystals were obtained in two days.

Yield: 0.45 g, 75%. *Anal.* Calc. for  $\text{C}_{22}\text{H}_{30}\text{Cu}_2\text{N}_{10}\text{O}_2$  (**1**): C, 44.51; H, 5.09; N, 23.59. Found: C, 44.47; H, 5.15; N, 23.55%. IR (KBr pellet,  $\text{cm}^{-1}$ ): 3436 (broad)  $\nu(\text{OH})$ , 3181  $\nu(\text{NH})$ , 2045  $\nu(\text{N}=\text{N})$  1620  $\nu(\text{C}=\text{N})$ ,  $\lambda_{\text{max}}$  (methanol), 606 nm.

### 2.3. Synthesis of $[\text{Cu}_2\text{L}_2(\text{N}_3)_2](\text{H}_2\text{O})$ (**2**)

The procedure was the same as that for complex **1**, except that triethylamine (0.28 mL, 2 mmol) was added to the reaction mixture after the addition of  $\text{NaN}_3$  solution. The bluish-green X-ray quality, plate shaped single crystals were obtained from the resulting blue solution on keeping overnight.

Yield: 0.50 g, 80%. *Anal.* Calc. for  $\text{C}_{22}\text{H}_{32}\text{Cu}_2\text{N}_{10}\text{O}_3$  (**2**): C, 43.20; H, 5.27; N, 22.90. Found: C, 43.27; H, 5.25; N, 22.85%. IR (KBr pellet,  $\text{cm}^{-1}$ ): 3244  $\nu(\text{NH})$ , 2044  $\nu(\text{N}=\text{N})$  1625  $\nu(\text{C}=\text{N})$ ,  $\lambda_{\text{max}}$  (methanol), 599 nm.

### 2.4. Synthesis of $[\text{CuL}(\text{N}_3)]_n$ (**3**)

The procedure was the same as that used for complex **1** except that a methanol–water solution (9:1, v/v) of excess  $\text{NaN}_3$  (0.260 g, 4 mmol) was added with slow stirring. The solution was left to stand overnight in air to yield needle shaped deep green X-ray quality single crystals of complex **3**.

Yield: 0.22 g, 73%. *Anal.* Calc. for  $\text{C}_{11}\text{H}_{15}\text{CuN}_5\text{O}$  (**3**): C, 44.51; H, 5.09; N, 23.59. Found: C, 44.45; H, 5.13; N, 23.63%. IR (KBr pellet,  $\text{cm}^{-1}$ ): 3245  $\nu(\text{NH})$ , 2043  $\nu(\text{N}=\text{N})$  1624  $\nu(\text{C}=\text{N})$ ,  $\lambda_{\text{max}}$  (methanol), 606 nm.

### 2.5. Physical measurements

Elemental analyses (C, H and N) were performed using a Perkin-Elmer 240C elemental analyzer. IR spectra in KBr pellets (4500–500  $\text{cm}^{-1}$ ) were recorded using a Perkin-Elmer RXI FT-IR spectrophotometer. Electronic spectra in methanol (1000–200 nm) were recorded in a Hitachi U-3501 spectrophotometer. Thermal analyses (TG-DTA) were carried out on a Mettler Toledo TGA/SDTA 851 thermal analyser in a dynamic atmosphere of dinitrogen (flow rate = 30  $\text{cm}^3 \text{min}^{-1}$ ). The samples were heated in an alumina crucible at a rate of 10  $^\circ\text{C} \text{min}^{-1}$ . The magnetic susceptibility measurements were carried out in the temperature range 2–300 K with an applied magnetic field of 0.5 T on polycrystalline samples of compounds **1–3** (with masses of 45.70, 56.69 and 34.63 mg, respectively) with a Quantum Design MPMS-XL-5 SQUID susceptometer (PPMS-9 equipment for sample **3**). The isothermal magnetizations were performed on the same samples at 2 K with magnetic fields up to 5 T (up to 8 T in PPMS-9 equipment for sample **3**). The susceptibility data were corrected for the sample holders previously measured using the same conditions and for the diamagnetic contributions of the salts as deduced by using Pascal's constant tables ( $\chi_{\text{dia}} = -345.4 \times 10^{-6}$ ,  $-354.7 \times 10^{-6}$  and  $-172.7 \times 10^{-6} \text{ emu mol}^{-1}$  for **1–3**, respectively).

**Table 1**  
Crystal and refinement data for compounds **1** and **2**.

Compound	<b>1</b>	<b>2</b>
Formula	$\text{C}_{22}\text{H}_{30}\text{Cu}_2\text{N}_{10}\text{O}_2$	$\text{C}_{22}\text{H}_{32}\text{Cu}_2\text{N}_{10}\text{O}_3$
Formula weight	593.66	611.68
Temperature (K)	150	150
Space group	$P\bar{1}$	$P\bar{1}$
Crystal system	triclinic	triclinic
<i>a</i> (Å)	7.658(1)	7.8575(6)
<i>b</i> (Å)	8.952(4)	9.6622(6)
<i>c</i> (Å)	9.619(3)	17.6571(8)
$\alpha$ ( $^\circ$ )	103.07(3)	81.285(6)
$\beta$ ( $^\circ$ )	96.25(2)	79.946(6)
$\gamma$ ( $^\circ$ )	101.83(3)	75.217(6)
<i>V</i> (Å <sup>3</sup> )	620.3(3)	1268.18(16)
<i>Z</i>	1	2
<i>D</i> <sub>calc</sub> (g/cm <sup>3</sup> )	1.589	1.602
$\mu$ (mm <sup>-1</sup> )	1.756	1.723
<i>F</i> (0 0 0)	306	632
Total reflections	4431	8980
Unique reflections	3480	7078
Observed data [ <i>I</i> > 2 $\sigma$ ( <i>I</i> )]	2564	5105
Number of parameters refined	164	342
<i>R</i> <sub>int</sub>	0.0300	0.0240
<i>R</i> indices (all data)	<i>R</i> <sub>1</sub> = 0.0414 <i>wR</i> <sub>2</sub> = 0.0843	<i>R</i> <sub>1</sub> = 0.0362 <i>wR</i> <sub>2</sub> = 0.0802

## 2.6. Crystal data collection and refinement

Crystal data for complexes **1** and **2** are given in Table 1. 3480, and 7078 independent data for **1** and **2** were collected with Mo K $\alpha$  radiation at 150 K using an Oxford diffraction X-calibur CCD system. The crystals were positioned at 50 mm from the CCD. 321 frames were measured with a counting time of 10 s. Data analysis was carried out with the CRYSLIS program [32]. The structures were solved using direct methods with the SHELXS97 program [33]. The non-hydrogen atoms were refined with anisotropic thermal parameters. The hydrogen atoms bonded to carbon were included in geometric positions and given thermal parameters equivalent to 1.2 times (or 1.5 times for methyl hydrogen atoms) those of the atom to which they were attached. The hydrogen atoms bonded to the water molecule in **2** were located in a difference Fourier map and refined with distance constraints. Empirical absorption corrections were carried out with ABSPACK [34]. The structures were refined on  $F^2$  using SHELXL97 [33] to  $R_1$  values 0.0362 and 0.0414;  $wR_2$  values 0.0843 and 0.0802 for 2564 and 5105 reflections with  $I > 2\sigma(I)$  for complexes **1** and **2**, respectively.

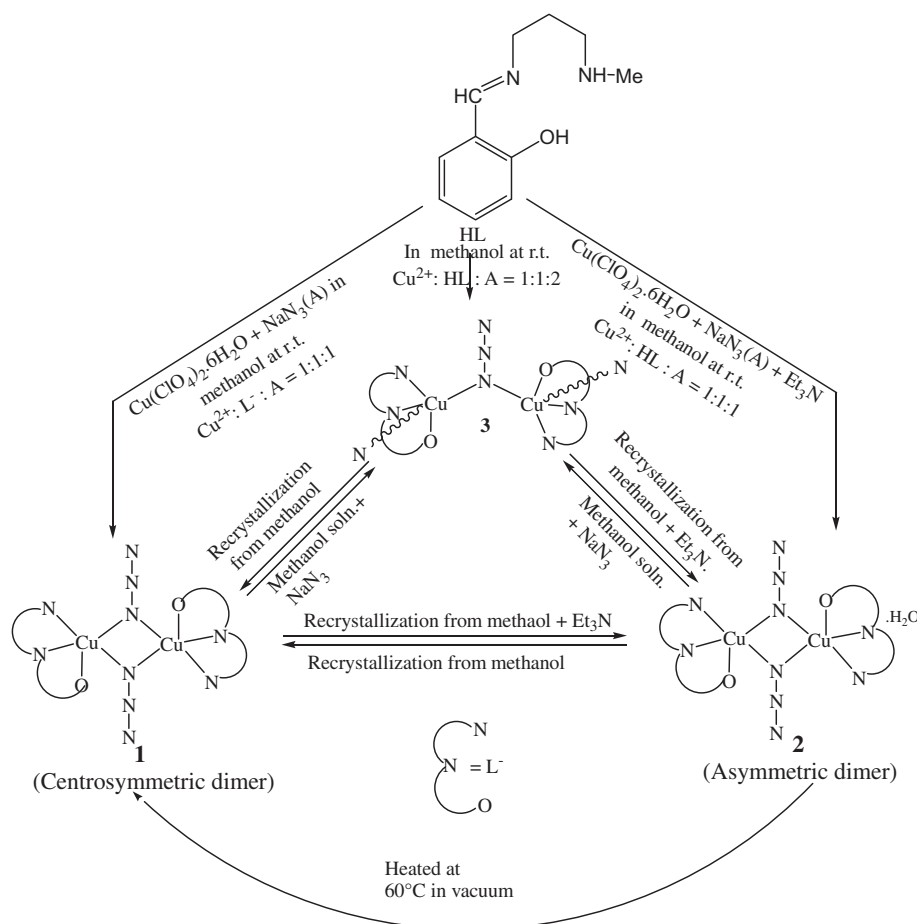
## 3. Results and discussion

### 3.1. Synthesis of the complexes and their inter-conversion in solution

The mono-condensed tridentate Schiff base ligand HL and its hydroxo-bridged trinuclear complex obtained with Cu(II) and  $\text{ClO}_4^-$  anion, has already been reported by us very recently [35].

In the present investigation we have used this ligand for the synthesis of complexes with Cu(II) and  $\text{N}_3^-$  anions. This group of mono negative N,N,O donor ligands usually produce double asymmetric [ $\mu$ -1,1-azide-bridged dimers like complex **1** which has been prepared by reacting a methanolic solution of  $\text{Cu}(\text{ClO}_4)_2 \cdot 6\text{H}_2\text{O}$  with a methanolic solution of HL followed by the addition of an aqueous solution of  $\text{NaN}_3$  in 1:1:1 molar ratio. Compound **2** on the other hand crystallized when triethylamine was added to the reaction mixture. Compound **2** transforms into compound **1** on recrystallization from methanol whereas addition of a few drops of triethylamine to a methanolic solution of **1** followed by slow evaporation of the solvent yields compound **2** (see Scheme 2).

On the other hand, when a methanolic solution of HL and  $\text{Cu}(\text{ClO}_4)_2 \cdot 6\text{H}_2\text{O}$  is allowed to react with excess azide ions in the molar ratio 1:1:2 at room temperature, the 1D polymer  $[\text{Cu}_2\text{N}_3]_n$  (**3**), which is held together by single  $\mu$ -1,1-azide bridges, is obtained. Compounds **1** and **2** also convert easily into **3**; when a methanol-water (9/1, v/v) solution of sodium azide is added to a methanolic solution of **1** or **2** (1:1 molar ratio or more), compound **3** starts to crystallize within an hour. The higher concentration of azide ion seems to be the driving force for its formation. Again, compound **3** transforms into compound **1** on recrystallization from methanol and into **2** when few drops of triethylamine are added to the methanol solution (see Scheme 2). From these experimental observations, it is clear that compound **1** crystallizes from neutral methanolic solution, **2** from a solution containing triethylamine and **3** in presence of excess azide ions. It is to be noted that com-



Scheme 2. Synthetic route of **1**–**3**.

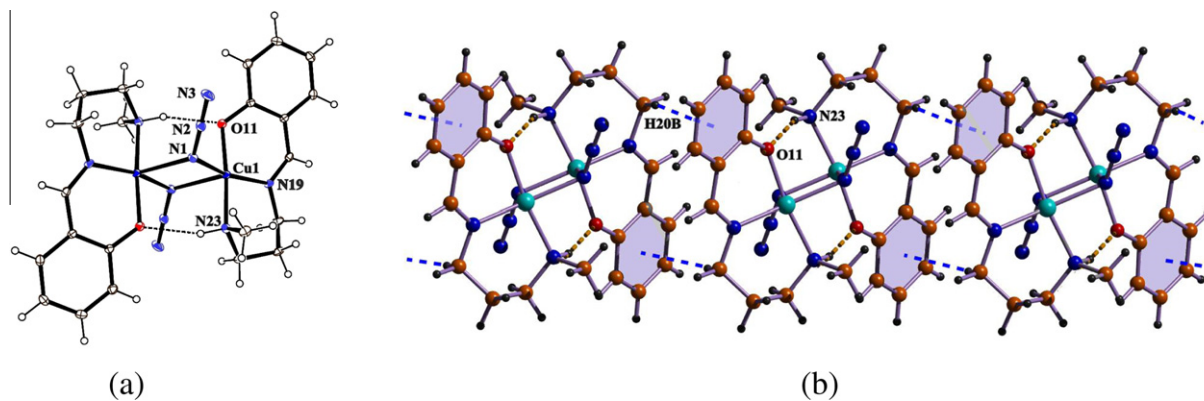


**Fig. 1.** (a) Structure of **1** with ellipsoids at 30% probability. Hydrogen bonds shown as dotted lines. (b) Polymeric 1D structure of **1** formed by the interdimer C–H/ $\pi$  interactions, shown as blue coloured dotted lines. (For interpretation of the references to colour in this figure legend, the reader is referred to the web version of this article.)

compound **3** has been synthesised recently using ethanol as solvent and a similar compound to **1** in which methanol was the solvent molecule, has been obtained using methanol as solvent [28].

### 3.2. Solid state transformation of **2** to **1**

Transformation of compound **2** to **1** takes place not only in solution but also in the solid state. From the X-ray structure it is found that the guest water molecule is stabilized by hydrogen bonds in between two dimeric entities in compound **2**. Upon heating at 60 °C in a high vacuum autoclave, bluish green crystals of **2** turn into deep blue (Figure S1). However, on heating, the single crystal of **2** turns opaque after losing one water molecule and it does not diffract indicating that the single crystallinity is not retained on thermal desolvation. The powder XRD data (Figure S2) indicate that complex **2** on heating transform to **1** on losing the solvated water molecule. The thermogravimetric analysis shows a weight loss of 3.0% in the temperature range 60–90 °C, corresponding to the loss of one crystallization water molecule (calc. 2.9%) (Figure S3). The dehydrated sample on exposure to open atmosphere does not reabsorb the water molecule. Therefore, it is clear that

compound **2** upon dehydration undergoes irreversible solid state transformation into **1**.

Solid state transformation from one state to other is a fast-emerging topic in chemical sciences especially in solid-state synthesis and crystal engineering. Such a phenomenon has potential applications in catalysis, magnetism, and in the design of solid-state sensors. However, inorganic coordination complexes showing crystal-to-crystal transformations are scanty because these transformations imply the cooperative movement of atoms or molecules in the solid state, leading to the loss of structural identity. Most of the known examples are 3D and 2D coordination polymers with high stability and porous crystalline structures in which the crystal transitions are usually triggered by light, temperature, guest desorption/adsorption or ion exchange [40–46]. In the present case, although the single crystallinity of **2** is lost on dehydration, we were able to get the crystals of **2** from solution by varying the reaction conditions.

### 3.3. IR and UV–Vis spectra of complexes

Spectroscopic data and their assignments are given in Section 2. The IR spectra of the complexes are similar and show a strong and sharp peak for  $\nu(\text{C}=\text{N})$  at 1620, 1625 and 1624  $\text{cm}^{-1}$  for complexes **1–3**, respectively, indicating the presence of the Schiff base. The N–H stretching mode is seen at 3181, 3244 and 3245  $\text{cm}^{-1}$  as a sharp band for complexes **1–3**, respectively. The peaks at 2045, 2044 and 2043  $\text{cm}^{-1}$  in the IR spectra of **1–3**, respectively, appear due to the stretching of the  $\mu$ -1,1 single or double azide bridges. In the IR spectra of complex **2**, the appearance of a broad band near 3436  $\text{cm}^{-1}$  indicates the presence of a hydrogen bonded water molecule, consistent with the single-crystal X-ray diffraction results. The electronic spectra in methanolic solution of the three complexes display a single absorption band at 606, 599 and

**Table 2**  
Bond distances (Å) and angles (°) for compounds **1** and **2**.

	<b>1</b>	<b>2</b>	
	X = N(1) <sup>a</sup>	Around Cu(1) X = N(4)	Around Cu(2) <sup>a</sup> X = N(4)
<i>Bond distances</i>			
Cu(1)–O(11)	1.924(2)	1.908(2)	1.910(2)
Cu(1)–N(19)	1.997(2)	1.979(2)	1.969(2)
Cu(1)–N(23)	2.021(2)	2.023(2)	2.033(2)
Cu(1)–N(1)	2.059(2)	2.354(2)	2.339(2)
Cu(1)–X	2.338(2)	2.060(2)	2.045(2)
<i>Bond angles</i>			
O(11)–Cu(1)–N(19)	90.95(9)	90.85(7)	92.39(7)
O(11)–Cu(1)–N(23)	172.12(8)	166.46(7)	159.30(7)
O(11)–Cu(1)–X	89.84(8)	96.56(7)	100.78(7)
O(11)–Cu(1)–N(1)	86.46(9)	86.50(7)	89.33(7)
N(19)–Cu(1)–N(23)	96.68(9)	93.93(8)	92.09(8)
N(19)–Cu(1)–X	109.26(8)	108.42(7)	102.20(7)
N(19)–Cu(1)–N(1)	162.52(9)	171.69(8)	176.56(8)
N(23)–Cu(1)–X	89.49(8)	93.94(7)	97.99(7)
N(23)–Cu(1)–N(1)	85.67(9)	86.98(8)	85.27(8)
N(1)–Cu(1)–X	88.04(9)	79.73(7)	80.40(7)
Cu(1)–N(1)–Cu(2)	91.95(9)	97.87(8)	97.93(9)

Symmetry code,  $' = 1 - x, 2 - y, 1 - z$ .

<sup>a</sup> Dimensions around Cu(2) are given alongside the equivalent dimensions around Cu(1). The coordination sphere around Cu(2) contains atoms O(31), N(39), N(43), N(4) and N(1), respectively.

**Table 3**  
Hydrogen bonds parameters (in Å and °) in compounds **1** and **2** (D = donor, A = acceptor).

	D...A	H...A	<D–H...A	Symmetry element for A
<i>Compound 1</i>				
N(23)–H...O(11)	2.982(3)	2.11	161	$1 - x, 2 - y, 1 - z$
<i>Compound 2</i>				
N(43)–H...O(11)	2.914(2)	2.21	134	
O(100)–H(1)...N(6)	3.107(3)	2.34	154	$2 - x, 2 - y, 1 - z$
O(100)–H(2)...O(31)	2.722(2)	1.90	173	
N(23)–H...O(100)	2.978(3)	2.10	162	

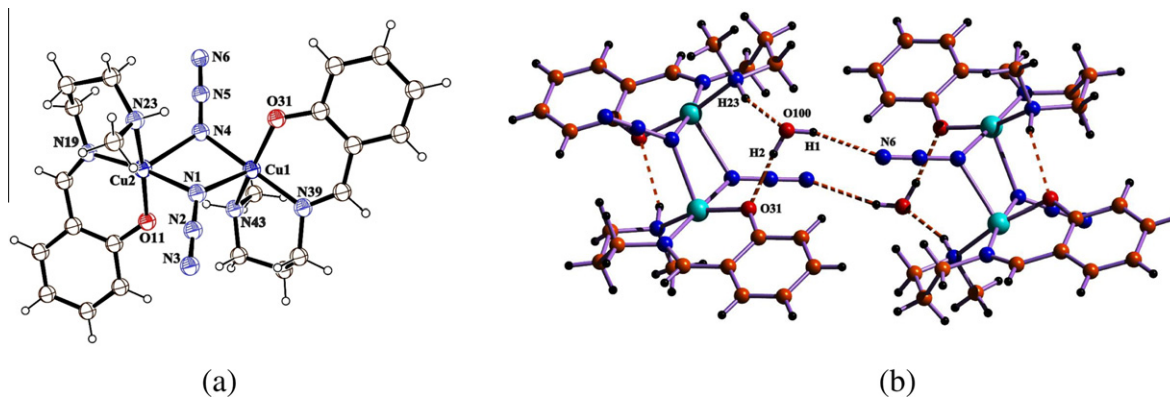


**Fig. 2.** (a) The Cu(II) dinuclear structure of **2** with ellipsoids drawn at 30% probability. (b) The hydrogen bonding network. Hydrogen bonds are shown as dotted lines.

606 nm for complexes **1–3**, respectively. These spectra are typical of a square-based environment for Cu(II) [47].

### 3.4. Description of the structures

#### 3.4.1. Structure of $[Cu_2L_2(N_3)_2]$ (**1**)

The structure of **1** consists of a centrosymmetric Cu(II) dimer with a double  $\mu$ -1,1-azido bridge (Fig. 1). Dimensions in the metal coordination sphere are given in Table 2.

The Cu(II) ion shows a five-coordinate square pyramidal environment with the tridentate ligand and with one bridging azide in the basal plane and a further bridging azide in an axial site. Each azide ion bridges the Cu(II) ions in basal-apical,  $\mu$ -1,1 (end-on) fashion. The di- $\mu$ -1,1-azido bridging in these complexes leads to a perfectly planar  $Cu_2N_2$  ring as the dimer sits on a crystallographic inversion centre with a Cu–N–Cu bond angle of  $91.96(9)^\circ$ . The four donor atoms in the basal plane exhibit a tetrahedral distortion with an r.m.s. (root means square) deviation of  $0.146 \text{ \AA}$  from planarity with the copper atom located  $0.159(1) \text{ \AA}$  above the average plane, towards the axial bond. The bond length involving the axial azide is  $2.338(2) \text{ \AA}$ , much longer than that of the basal azide  $2.059(2) \text{ \AA}$ . Bond lengths to the ligand are Cu(1)–O(11) =  $1.924(2) \text{ \AA}$ , Cu(1)–N(19) =  $1.997(2) \text{ \AA}$  and Cu(1)–N(23) =  $2.021(2) \text{ \AA}$ . The Addison parameter value for complex **1** ( $\tau = 0.16$ ), confirms the distorted square pyramidal structure for the Cu(II) ion. ( $\tau$  is defined as  $|\beta - \alpha|/60$  where  $\beta$  and  $\alpha$  are the two trans-basal angles, with  $\tau = 0$  and 1 for perfect square pyramid and trigonal bipyramid geometries, respectively) [48]. The coordinated azide ion is nearly linear with a N(1)–N(2)–N(3) angle of  $178.5(5)^\circ$ . The formation of the centrosymmetric dimer is facilitated by hydrogen bonds from N(23)–H to O(11) across the centre of symmetry with  $N \cdots O = 2.982(3) \text{ \AA}$  (Fig. 1b, Table 3). In addition, a C–H/ $\pi$  non-covalent interaction is established between the H(20B) atom of the Schiff base ligand belonging to one dinuclear unit and the aromatic ring of the neighbouring one ( $1 - x, 1 - y, 1 - z$ ) with dimensions  $H \cdots Cg = 2.63 \text{ \AA}$ , gamma angle ( $\gamma$ ) =  $6.29^\circ$  to form a supra-molecular 1D architecture (Fig. 1b).

#### 3.4.2. Structure of $[Cu_2L_2(N_3)_2(H_2O)]$ (**2**)

The structure of **2** is shown in Fig. 2a together with the atomic numbering scheme. This compound has the same overall structure as **1** but the dimer is asymmetric and there is one water molecule per Cu(II) dimer. This water molecule is inserted within the dimer forming a hydrogen bond (as a donor) to O(31) and as an acceptor with N(23) (Fig. 2b, Table 3). Bond distances and angles are listed in Table 2. The presence of the water molecule means that there is no direct hydrogen bond between N(23) and O(31). Indeed the distance has increased to  $4.279(4) \text{ \AA}$  compared to  $2.982(3) \text{ \AA}$  in **1**.

The hydrogen bond between N(43) and O(11), is however maintained with a distance of  $2.914(2) \text{ \AA}$  comparable to that in **1**. The Addison parameters for Cu1 and Cu2 are 0.09 and 0.29, respectively. As in compound **1**, the basal planes of the Cu(II) ions are formed by the N,N,O-Schiff base ligand with Cu–O and Cu–N bond distances very similar to those of compound **1** (see Table 2).

The azide ions are nearly linear with N(1)–N(2)–N(3) and N(4)–N(5)–N(6) angles of  $178.6(2)^\circ$  and  $177.7(3)^\circ$ , respectively. The four donor atoms in the basal plane show tetrahedral distortions with r.m.s. deviations of  $0.034$  and  $0.149 \text{ \AA}$  from planarity for Cu(1) and Cu(2), respectively, being the copper atoms  $0.177(1)$  and  $0.195(1) \text{ \AA}$  above the averages planes in the direction of the axial bonds. The dihedral angle between the two basal planes in **2** is  $10.7(1)^\circ$ , higher than in compound **1** (where the angle is  $0.0^\circ$  since the compound is centrosymmetric). Another interesting difference between compounds **1** and **2** is that in **2** the central  $Cu_2N_2$  unit is not planar (in contrast to **1**). The deviations of the four atoms from the mean plane passing through Cu(1)–Cu(2)–N(1)–N(4) are  $0.144$ ,  $0.146$ ,  $-0.145$  and  $-0.145 \text{ \AA}$ , respectively. As a consequence of this asymmetry, the two bridging Cu–N–Cu angles and the four Cu–N distances are slightly different (Table 2).

#### 3.4.3. Structure of $[CuL(N_3)]_n$ (**3**)

As mentioned earlier, structure of **3** has already been reported. So we do not describe the structural part here. The ORTEP diagram (S4) and the table (S5) for bond angle and distances are presented as supporting information.

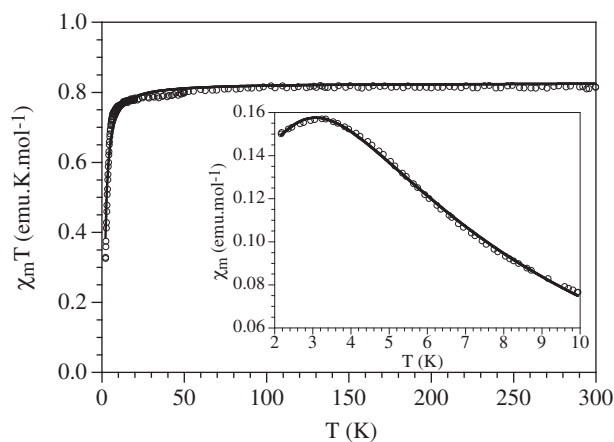


**Fig. 3.** Thermal variation of the  $\chi_m T$  product per Cu(II) dimer for compound **1**. Inset shows the thermal variation of  $\chi_m$  in the low temperature region. Solid line shows the best fit to the  $S = 1/2$  dimer model (see text).

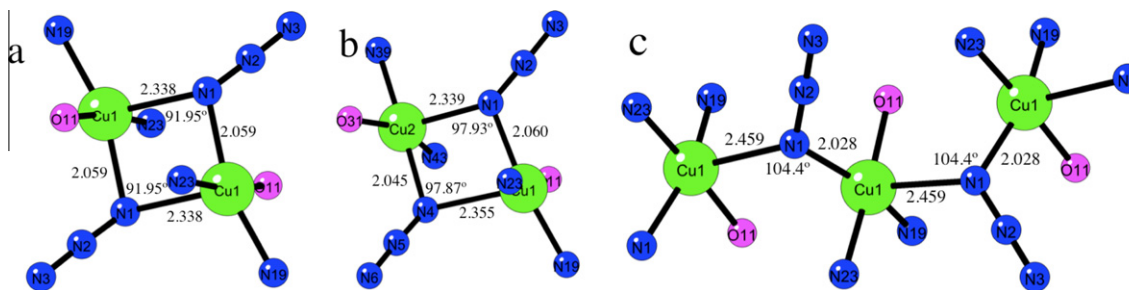


**Fig. 4.** Coordination environment of the Cu(II) ions in compounds (a) **1**, (b) **2** and (c) **3** showing the bridging bond distances (in Å) and angles (in degrees). Colour code: Cu = green, N = blue, O = pink. (For interpretation of the references to colour in this figure legend, the reader is referred to the web version of this article.)

**Table 4**  
Structural and magnetic parameters of compounds **1–3**.

	Structure	Bridge	Cu–N (Å)	Cu–N–Cu (°)	<i>g</i>	<i>J</i> (cm <sup>−1</sup> )
1	Cu-dimer	Double 1,1-N <sub>3</sub> (asymmetric)	2.059/2.338	91.95(9)	2.0999	−2.59
2	Cu-dimer	Double 1,1-N <sub>3</sub> (asymmetric)	2.045/2.355	97.87(8)	2.0666	−0.10
			2.060/2.339	97.93(9)		
3	Cu-chain	Single 1,1-N <sub>3</sub> (asymmetric)	2.028/2.459	104.4(4)	2.0931	−0.01

It is noteworthy to recall that although there are ca. 30 Cu(II)  $\mu$ -1,1-azido bridged dimers reported in the literature, only the recently reported [28] complex related to **2** and compound **2** are non-centrosymmetric, being all the other centrosymmetric, as compound **1** [25–27,29,30]. On the other hand, single  $\mu$ -1,1 (end-on) azido bridged Cu(II) complexes, like **3**, are also rare. A search in the CCDC database (updated Feb. 2011) shows the presence of only three such complexes reported to date. One is a trimer [48] and the other two are 1-D chains, as indeed is complex **3** [49–51].

### 3.5. Magnetic properties

The thermal variation of the molar magnetic susceptibility per two Cu(II) ions times the temperature ( $\chi_m T$ ) for compounds **1** and **2** are very similar: they show values of ca. 0.82 and 0.80 emu K mol<sup>−1</sup> at room temperature for **1** and **2**, respectively, the expected ones for two isolated Cu(II)  $S = 1/2$  ions with  $g = 2.09$  and 2.06, respectively (Figs. 3 and 6). When cooling down the sample, the  $\chi_m T$  product remains constant down to ca. 20 and 10 K for **1** and **2**, respectively and below these temperatures,  $\chi_m T$  shows a smooth and progressive decrease, reaching values of ca. 0.32 and 0.78 emu K mol<sup>−1</sup> at 2 K for **1** and **2**, respectively. This behaviour indicates that compounds **1** and **2** present very weak antiferromagnetic coupling, responsible of the decrease observed at low temperatures (although that of compound **1** must be stronger than in compound **2**). In compound **1** this weak antiferromagnetic coupling is also observed in the thermal variation of  $\chi_m$  that shows a rounded maximum at ca. 3 K (inset in Fig. 3).

Since compounds **1** and **2** present isolated Cu(II) dimers with a double asymmetric 1,1-N<sub>3</sub> bridge (Fig. 4a and 4b), we have used a simple Bleaney–Bowers dimer model for two  $S = 1/2$  ions to fit the magnetic data [52,53]. This model reproduces very satisfactorily the magnetic properties of both compounds in the whole temperature range (solid lines in Figs. 3 and 6) with  $g = 2.0999(2)$  and  $J = -2.59(4)$  cm<sup>−1</sup> for **1** and  $g = 2.0666(3)$  and a negligible  $J$  value of  $-0.10(1)$  cm<sup>−1</sup> for **2** (Table 4, the Hamiltonian is written as  $H = -JS_1S_2$ ).

The isothermal magnetization measurements at 2 K (Fig. 5) confirm the presence of a weak antiferromagnetic coupling in compound **1** and an almost negligible one in compound **2**. Thus, at 2 K, compound **1** has not reached saturation at 5 T (nor even at

8 T, not shown) and shows a value at 8 T of ca. 1.6  $\mu_B$  per Cu(II) dimer, below the expected one for two isolated Cu(II) ions with  $g = 2$ . In fact, the Brillouin function for two isolated Cu(II) ions cannot reproduce satisfactorily the isothermal magnetization unless the temperature,  $T$  is replaced by a reduced  $T - \theta$  term to account for the antiferromagnetic intra-dimer coupling (solid line in Fig. 5). In contrast, compound **2** shows an isothermal magnetization at 2 K close to the expected one for a paramagnetic  $S = 1/2$  dimer with a saturation value close to 2.0  $\mu_B$  per Cu(II) dimer and can be very well reproduced with a Brillouin function for two isolated  $S = 1/2$  ions (solid line in Fig. 5).

The product of the molar magnetic susceptibility per Cu(II) ion times the temperature ( $\chi_m T$ ) for compound **3** shows at room temperature a value of ca. 0.41 emu K mol<sup>−1</sup>, which is the expected value for one isolated Cu(II)  $S = 1/2$  ions with  $g = 2.09$  (Fig. 7). When cooling down the sample, the  $\chi_m T$  product remains constant down to very low temperatures, indicating that compound **3** is also essentially paramagnetic, as confirmed by the fit of the magnetic properties to a simple  $S = 1/2$  regular antiferromagnetic chain model [54] in agreement with the structure of **3** (Fig. 4c). This

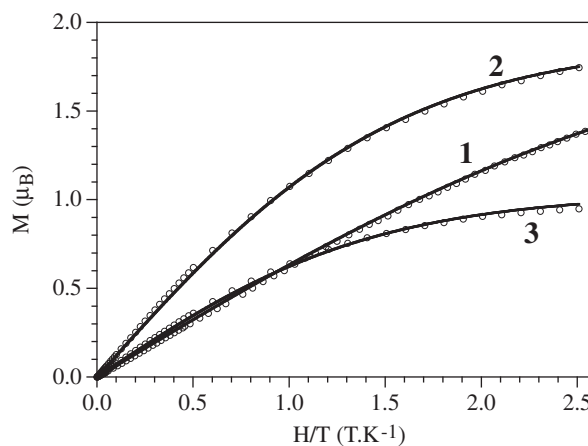


**Fig. 5.** Isothermal magnetizations at 2 K for compounds **1–3**. Solid lines are the best fit to the modified Brillouin function for the corresponding  $S = 1/2$  ions (two for **1** and **2** and one for **3**).

simple model reproduces quite satisfactorily the magnetic data of compound **3** in the whole temperature range (solid line in Fig. 7) with  $g = 2.0931(1)$  and a negligible antiferromagnetic coupling,  $J = -0.010(4) \text{ cm}^{-1}$  (Table 4, the Hamiltonian is written as  $H = -JS_1S_2$ ).

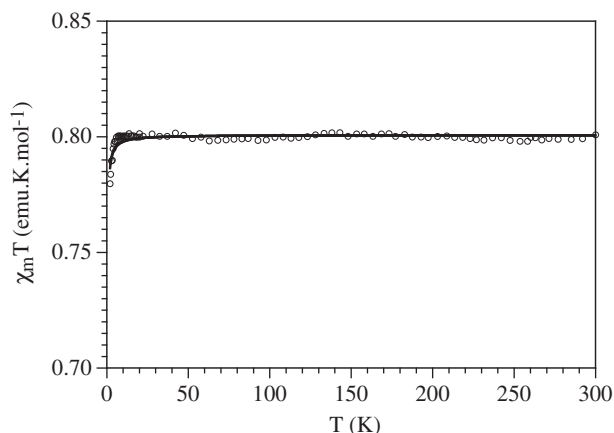


Fig. 6. Thermal variation of the  $\chi_m T$  product per Cu(II) dimer for compound **2**. Solid line shows the best fit to the  $S = 1/2$  dimer model (see text).

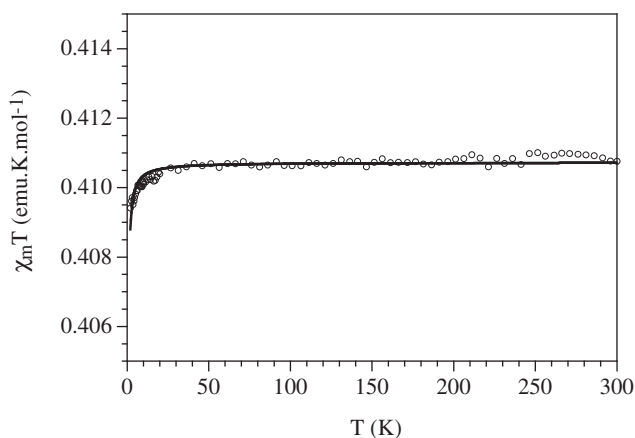


Fig. 7. Thermal variation of the  $\chi_m T$  product per Cu(II) ion for compound **3**. Solid line shows the best fit to the  $S = 1/2$  chain model (see text).

The isothermal magnetization of compound **3** at 2 K shows a saturation value close to  $1.0 \mu_B$ , the expected value for an  $S = 1/2$  Cu(II) ion with a  $g$  value close to 2.0 and it can be very well reproduced with a Brillouin function for an  $S = 1/2$  ion, confirming the paramagnetic behaviour of compound **3** (solid line in Fig. 5).

The magnetic couplings in compounds **1–3** can be very well rationalized with the magneto-structural correlations and theoretical calculations performed for single and double asymmetric 1,1- $N_3$  bridges [27]. Thus, DFT calculations show that the main parameter governing the magnetic coupling through asymmetric double 1,1- $N_3$  bridges (as observed in **1** and **2**) is the long Cu–N bond distance. These calculations indicate that for compounds **1** and **2**, where the 1,1- $N_3$  bridges connect an axial position of one Cu(II) ion with a basal position of the other one, the expected coupling should be antiferromagnetic and very weak, in agreement with the experimental  $J$  values. If we compare both structures in order to explain the differences found in the coupling constants, we can see that the Cu(II) ions in both complexes present slightly distorted square pyramidal geometries with an Addison parameter in compound **1** ( $\tau = 0.16$ ) which is in between the  $\tau$  values of Cu(1) and Cu(2) in compound **2** ( $\tau = 0.09$  and  $0.29$ ). Furthermore, the 1,1- $N_3$  bridges connect in both cases an axial position of one Cu(II) ion with a basal position of the other one and the Cu–N bond distances are also very similar (Table 4 and Fig. 4a and b). In fact, the only significant difference is the Cu–N–Cu bond angle. Thus, in compound **2** the Cu–N–Cu bond angles are much larger ( $97.87^\circ$  and  $97.93^\circ$ ) than the corresponding one in compound **1** ( $91.95^\circ$ ). This situation leads to a better overlap of the orbitals in compound **1** and, therefore, to a larger antiferromagnetic coupling in compound **1**, in agreement with the experimental results.

Unfortunately, for the single asymmetric 1,1- $N_3$  bridges there are neither magneto-structural correlations nor calculations since there are few examples and these examples do not show any correlation between the magnetic coupling and any structural parameter (in particular neither Cu–N bond distances nor Cu–N–Cu bond angles, Table 5). In any case, all the reported examples show a weak magnetic coupling (mainly antiferromagnetic, with  $J$  values in the range  $-0.12$  and  $-4.06 \text{ cm}^{-1}$ , except in one case, where  $J = -11.4 \text{ cm}^{-1}$ , probably due to an unusual short Cu–N long distance of  $2.276 \text{ \AA}$ , compared to  $2.343$ – $2.598 \text{ \AA}$  in all the other examples, see Table 5). In summary, the negligible antiferromagnetic coupling found in compound **3** is within the expected range for this type of 1,1- $N_3$  bridge even if the exact value of this coupling is difficult to predict from structural parameters.

Table 5

Magnetic and structural data of the known compounds presenting Cu(II) ions connected by single asymmetric  $\mu$ -1,1- $N_3$  bridges.

Compound (CCDC code)	Positions	Cu–N (Å)	Cu–N–Cu ( $^\circ$ )	$J$ ( $\text{cm}^{-1}$ )	Reference
FISFAP	Ax( $C_{4v}$ )	2.305(4)-ax	117.4(2)	+2.88	[55]
	Eq( $C_{4v}$ )	1.991(5)-eq			
FODQJZ	Ax( $C_{4v}$ )	2.343(4)-ax	130.78(19)	–4.06	[56]
	Eq( $C_{4v}$ )	2.044(4)-eq			
GAMVOG	Ax( $C_{4v}$ )	2.416(2)-ax	113.6(1)	–2.2	[57]
	Eq( $C_{4v}$ )	1.961(2)-eq			
GAMVUM	Ax( $C_{4v}$ )	2.598(2)-ax	107.01(10)	–3.7	[58]
	Eq( $C_{4v}$ )	1.951(2)-eq			
IQASEY	Ax( $C_{4v}$ )	2.341(2)-ax	116.60(9)	+14.1	[17]
	Eq( $C_{4v}$ )	1.992(2)-eq			
KAKTOG	Ax( $C_{4v}$ )	2.480(4)-ax	126.33(19)	–0.21	[58]
	Eq( $C_{4v}$ )	1.994(4)-eq			
	Ax( $C_{4v}$ )	2.394(5)-ax			
VEVRET	Eq( $C_{4v}$ )	1.990(4)-eq	129.98(14)	–11.5	[59]
	Ax( $C_{4v}$ )	2.276(3)-ax			
WELPEJ	Eq( $C_{4v}$ )	2.007(2)-eq	131.6(4)	+1.91	[60]
	Ax( $C_{4v}$ )	2.342(9)-ax			
<b>3</b>	Eq( $C_{4v}$ )	1.983(9)-eq	104.4(4)	–0.01	This work
	Ax( $C_{4v}$ )	2.459(5)-ax			
	Eq( $C_{4v}$ )	2.028(5)-eq			

#### 4. Conclusions

By controlling the reaction conditions, a N,N,O-donor tridentate blocking Schiff base ligand has allowed the synthesis of two asymmetric double  $\mu$ -1,1-azido bridged Cu(II) dimers one of which is a usual centrosymmetric dimer whereas the other is a very unusual non-centrosymmetric dimer. Upon dehydration the non-centrosymmetric dimer  $[\text{Cu}_2\text{L}_2(\text{N}_3)_2]\cdot\text{H}_2\text{O}$  (**2**) undergoes a solid state transformation to generate the centrosymmetric dimer  $[\text{Cu}_2\text{L}_2(\text{N}_3)_2]$  (**1**). Variation of the reaction conditions affords a rare example of asymmetric single  $\mu$ -1,1-azido bridged chain polymer. The three complexes can easily be interconverted in solution. The structural analysis of **1** and **2** reveals that the only significant difference is the Cu–N–Cu bond angle, which is smaller in **1**. This situation leads to a better overlap of the orbitals in compound **1** and, therefore, to a relatively larger antiferromagnetic coupling in **1**, in agreement with the experimental results.

#### Acknowledgments

We thank CSIR, Government of India (Senior Research Fellowship to S.B. Sanction No. 09/028(0732)/2008-EMR-I), the European Union (MAGMANet Network of Excellence), the Spanish Ministerio de Educación y Ciencia (Projects CTQ2011-26507 and Consolider-Ingenio 2010 CSD 2007-00010 in Molecular Nanoscience) and the Generalitat Valenciana (Project PROMETEO/2009/095) for financial support. We also thank EPSRC and the University of Reading for funds for the X Calibur system.

#### Appendix A. Supplementary data

CCDC 810765, 810766 and 810767 contain the supplementary crystallographic data for compounds **1**, **2** and **3**, respectively. These data can be obtained free of charge from The Cambridge Crystallographic Data Centre via [www.ccdc.cam.ac.uk/data\\_request/cif](http://www.ccdc.cam.ac.uk/data_request/cif). Supplementary data associated with this article can be found in the online version, at [doi:10.1016/j.ica.2011.07.027](https://doi.org/10.1016/j.ica.2011.07.027).

#### References

- [1] M. Albrecht, *Chem. Rev.* 101 (2001) 3457.
- [2] R. Ziessel, *Coord. Chem. Rev.* 195 (2001) 216.
- [3] K.C. Gupta, A.K. Sutar, C.-C. Lin, *Coord. Chem. Rev.* 253 (2009) 1926.
- [4] D. Zhang, H. Wang, Y. Chen, Z.-H. Ni, L. Tian, J. Jiang, *Inorg. Chem.* 48 (2009) 11215.
- [5] P. Mukherjee, M.G.B. Drew, C.J. Gómez-García, A. Ghosh, *Inorg. Chem.* 48 (2009) 5848.
- [6] Q. Wang, J. Zhang, C.F. Zhuang, Y. Tang, C.Y. Su, *Inorg. Chem.* 48 (2009) 287.
- [7] B. Sarkar, M.S. Ray, Y.-Z. Li, Y. Song, A. Figuerola, E. Ruiz, J. Cirera, J. Cano, A. Ghosh, *Chem. Eur. J.* 13 (2007) 9297.
- [8] S. Chattopadhyay, M.G.B. Drew, C. Diaz, A. Ghosh, *Dalton Trans.* (2007) 2492.
- [9] C. Adhikary, S. Koner, *Coord. Chem. Rev.* 254 (2010) 2933.
- [10] K.C. Gupta, A.K. Sutar, *Coord. Chem. Rev.* 252 (2008) 1420.
- [11] K.L. Gurunatha, T.K. Maji, *Inorg. Chem.* 48 (2009) 10886.
- [12] T.K. Maji, G. Mostafa, R. Matsuda, S. Kitagawa, *J. Am. Chem. Soc.* 127 (2005) 17152.
- [13] E. Fujita, B.S. Brunschwig, T. Ogata, S. Yanagida, *Coord. Chem. Rev.* 132 (1994) 195.
- [14] S. Khatua, S.H. Choi, J. Lee, K. Kim, Y. Do, D.G. Churchill, *Inorg. Chem.* 48 (2009) 2993.
- [15] T. Kawamoto, M. Nishiwaki, Y. Tsunekawa, K. Nozaki, T. Konno, *Inorg. Chem.* 47 (2008) 3095.
- [16] T.C. Stamatatos, G.S. Papaefstathiou, L.R. MacGillivray, A. Escuer, R. Vicente, E. Ruiz, S.P. Perlepes, *Inorg. Chem.* 46 (2007) 8843.
- [17] E.-Q. Gao, S.-Q. Bai, C.-F. Wang, Y.-F. Yue, C.-H. Yan, *Chem.* 42 (2003) 8456.
- [18] G. Lazari, T.C. Stamatatos, C.P. Raptopoulou, V. Psycharis, M. Pissas, S.P. Perlepes, A.K. Boudalis, *Dalton Trans.* (2009) 3215.
- [19] S. Mukherjee, P.S. Mukherjee, *Inorg. Chem.* 49 (2010) 10658.
- [20] A.K. Boudalis, Y. Sanakis, J.M. Clemente-Juan, B. Donnadieu, V. Nastopoulos, A. Mari, Y. Coppel, J.-P. Tuchagues, S.P. Perlepes, *Chem. Eur. J.* 14 (2008) 2514.
- [21] K.C. Mondal, P.S. Mukherjee, *Inorg. Chem.* 47 (2008) 4215.
- [22] Z.-G. Gu, Y.-F. Xu, X.-J. Yin, X.-H. Zhou, J.-L. Zuo, X.-Z. You, *Dalton Trans.* (2008) 5593.
- [23] S. Mukherjee, B. Gole, R. Chakrabarty, P.S. Mukherjee, *Inorg. Chem.* 48 (2009) 11325.
- [24] C. Biswas, M.G.B. Drew, E. Ruiz, M. Estrader, C. Diaz, A. Ghosh, *Dalton Trans.* 39 (2010) 7474.
- [25] A. Escuer, M.A.S. Goher, F.A. Mautner, R. Vicente, *Inorg. Chem.* 39 (2000) 2107.
- [26] X.-Y. Song, W. Li, L.-C. Li, D.-Z. Liao, Z.-H. Jiang, *Inorg. Chem. Commun.* 10 (2007) 567.
- [27] S. Triki, C.J. Gómez-García, E. Ruiz, J. Sala-Pala, *Inorg. Chem.* 44 (2005) 5501.
- [28] L.-L. Ni, Z.-L. You, L.C. Wang, K. Li, *Transition. Met. Chem.* 35 (2010) 13.
- [29] A. Ray, S. Banerjee, R.J. Butcher, C. Desplanches, S. Mitra, *Polyhedron* 27 (2008) 2409.
- [30] M.S. Ray, A. Ghosh, R. Bhattacharya, G. Mukhopadhyay, M.G.B. Drew, J. Ribas, *Dalton Trans.* (2004) 252.
- [31] E. Ruiz, J. Cano, S. Alvarez, P. Alemany, *J. Am. Chem. Soc.* 120 (1998) 11122.
- [32] CRYSLIS, Oxford Diffraction Ltd., Abingdon, UK, 2006.
- [33] G.M. Sheldrick, *Acta Crystallogr., Sect. A* 64 (2008) 112.
- [34] ABSPACK, Oxford Diffraction Ltd., Oxford, UK, 2005.
- [35] S. Naiya, B. Sarkar, Y. Song, S. Ianelli, M.G.B. Drew, A. Ghosh, *Inorg. Chim. Acta* 363 (2010) 2488.
- [36] H. Lin, Y.L. Feng, S. Gao, *Chin. J. Struct. Chem.* 24 (2005) 375.
- [37] M.S. Ray, A. Ghosh, S. Chaudhuri, M.G.B. Drew, J. Ribas, *Eur. J. Inorg. Chem.* (2004) 3110.
- [38] J.P. Costes, F. Dahan, J. Ruiz, J.P. Laurent, *Inorg. Chim. Acta* 239 (1995) 53.
- [39] Z.-L. You, H.-L. Zhu, Z. Anorg. Allg. Chem. 630 (2004) 2754.
- [40] M. Kawano, M. Fujita, *Coord. Chem. Rev.* 251 (2007) 2592.
- [41] J.J. Vittal, *Coord. Chem. Rev.* 251 (2007) 1781.
- [42] O. Sengupta, Y. Song, P.S. Mukherjee, *Dalton Trans.* (2009) 10343.
- [43] J.-P. Zhao, B.-W. Hu, Q. Yang, T.-L. Hu, X.-H. Bu, *Inorg. Chem.* 48 (2009) 7111.
- [44] J. Seo, R. Matsuda, H. Sakamoto, C. Bonneau, S. Kitagawa, *J. Am. Chem. Soc.* 131 (2009) 12792.
- [45] A. Aslani, A. Morsali, *Chem. Commun.* (2008) 3402.
- [46] M. Albrecht, M. Lutz, A.L. Spek, G. van Koten, *Nature* 406 (2000) 970.
- [47] S. Naiya, C. Biswas, M.G.B. Drew, C.J. Gomez-García, J.M. Clemente-Juan, A. Ghosh, *Inorg. Chem.* 49 (2010) 6616.
- [48] A.W. Addison, T.N. Rao, J. Reedijk, J. Rijn, G.C. Verschoor, *J. Chem. Soc., Dalton Trans.* (1984) 1349.
- [49] Y.-B. Jiang, H.-Z. Kou, R.-J. Wang, A.-L. Cui, *Eur. J. Inorg. Chem.* (2004) 4608.
- [50] R. Bera, C. Adhikary, S. Ianelli, S. Chaudhuri, S. Koner, *Polyhedron* 29 (2010) 2166.
- [51] Z.-L. You, Q.-Z. Jiao, S.-Y. Niu, J.-Y. Chi, Z. Anorg. Allg. Chem. 632 (2006) 2481.
- [52] B. Bleaney, K.D. Blowers, *Proc. Roy. Soc. (London) Ser. A* 214 (1952) 451.
- [53] O. Kahn, *Molecular Magnetism*, VCH Publishers, 1993.
- [54] D.B. Brown, J.A. Donner, J.W. Hall, S.R. Wilson, R.B. Wilson, D.J. Hodgson, W.E. Hatfield, *Inorg. Chem.* 18 (1979) 2635.
- [55] X.-J. Lin, Z. Shen, Y. Song, H.-J. Xu, Y.-Z. Li, X.-Z. You, *Inorg. Chim. Acta* 358 (2005) 1963.
- [56] Z.-D. Wang, W. Han, F. Bian, Z.-Q. Liu, S.-P. Yan, D.-Z. Liao, Z.-H. Jiang, P. Cheng, *J. Mol. Struct.* 733 (2005) 125.
- [57] E.-Q. Gao, Y.-F. Yue, S.-Q. Bai, Z. He, C.-H. Yan, *Cryst. Growth Des.* 5 (2005) 1119.
- [58] H.-R. Wen, J.-L. Zuo, W. Liu, Y. Song, X.-Z. You, *Inorg. Chim. Acta* 358 (2005) 2565.
- [59] P.S. Mukherjee, T.K. Maji, G. Mostafa, T. Mallah, N.R. Chaudhuri, *Inorg. Chem.* 39 (2000) 5147.
- [60] S. Chattopadhyay, M.S. Ray, M.G.B. Drew, C. Diaz, A. Figuerola, A. Ghosh, *Polyhedron* 25 (2006) 2241.